Journal of Robotics and Control (JRC)
Volume 6, Issue 4, 2025
ISSN: 2715-5072, DOI: 10.18196/jrc.v6i4.25920

Modeling and Control of an 8-Legged Stewart Platform Using Null-Space Control for Precise Motion Under Actuator Constraints

Indrazno Siradjuddin [1], Ida Lailatul Fitria [2], Gillang Al Azhar [3], Septyana Riskitasari [4], Ferdian Ronilaya [5], Rendi Pambudi Wicaksono [6]
[1,2,3,5] Department of Electrical Engineering, State Polytechnic of Malang, Indonesia
[4] Department of Mechanical Engineering, State Polytechnic of Malang, Indonesia
[6] Department of Engineering, State Polytechnic of Madiun, Indonesia
Email: [1] indrazno@polinema.ac.id, [2] idalailatul25@gmail.com, [3] gillang_al_azhar@polinema.ac.id, [4] septyana_riskitasari@polinema.ac.id, [5] ferdian@polinema.ac.id, [6] rendipambudi@pnm.ac.id

Abstract*—This paper investigates the modeling, control, and redundancy resolution of an 8-legged Stewart platform, emphasizing the use of null-space control to achieve precise trajectory tracking while adhering to actuator constraints. The proposed control framework combines a Proportional-Integral-Derivative (PID) controller with null-space projection to exploit the platform's inherent redundancy for secondary objectives, such as singularity avoidance, energy optimization, and enhanced fault tolerance. A clamping strategy ensures that actuator lengths remain within operational limits, thereby preventing mechanical failures. Simulation results demonstrate significant error reduction in both position and orientation, even under strict actuator constraints. Specifically, the system achieved exponential convergence to the desired pose within $3\,$s, with a maximum position error of less than $1 \times 10^{-3}\,$m and orientation error below $5 \times 10^{-4}\,$rad. Actuator efficiency was also enhanced, as the algorithm dynamically redistributed efforts among actuators to avoid overloading any single leg. While energy consumption was not explicitly optimized in this study, the framework provides a foundation for future work in minimizing energy usage through advanced secondary objectives. Stability is analyzed rigorously using Lyapunov's direct method. Compared to traditional six-legged platforms, the 8-legged design offers superior flexibility and adaptability, making it particularly suitable for applications in flight simulators, robotic surgery, and industrial automation where precision and reliability are critical. However, the proposed approach has certain limitations. For instance, the current implementation assumes ideal actuator dynamics and does not account for uncertainties such as friction, backlash, or external disturbances. Additionally, the clamping strategy may introduce computational overhead, potentially impacting real-time performance in highly dynamic scenarios. Future research could address these limitations by incorporating adaptive or robust control techniques and optimizing computational efficiency. This work advances the design and control of redundant parallel manipulators, offering practical insights into dealing with physical limitations and providing a foundation for future innovations in high-performance motion control systems.

Keywords*—Stewart Platform; Null-Space Control; Redundancy Resolution; PID Control; Actuator Constraintsl; Lyapunov Stability; Simulation-Based Validation

I. Introduction

Parallel robotics, particularly the Stewart platform [1]–[20], has become a critical area in modern engineering due to its precision and stability. These platforms find applications in flight simulators, robotic surgery, and industrial automation [21]–[27]. However, controlling such systems poses challenges due to complex kinematic relationships and physical constraints, such as actuator length and velocity limits.

Redundancy, achieved by incorporating additional actuators (e.g., an eight-legged Stewart platform), enhances fault tolerance, flexibility, and singularity avoidance [28]–[32]. Nevertheless, redundancy complicates control design, as the system becomes over-actuated, resulting in an infinite number of solutions for achieving a desired pose. Most current studies focus on standard six-legged platforms, highlighting the need for research into effectively utilizing redundancy while ensuring robust operation.

Despite the potential benefits of redundancy, existing approaches for redundancy resolution in over-actuated systems face several limitations. For instance, many methods fail to adequately handle actuator constraints, leading to mechanical failures or suboptimal performance. Additionally, computational efficiency remains a challenge, particularly in real-time applications where rapid decision-making is essential. Existing techniques, such as optimization-based methods and task-priority frameworks, often prioritize theoretical elegance over practical applicability, making them less suitable for real-world scenarios. While these methods provide valuable insights, they frequently overlook the trade-offs introduced by redundancy, such as increased complexity in control algorithms and higher energy consumption. These trade-offs are crucial considerations in practical implementations, as they directly impact the feasibility and cost-effectiveness of deploying redundant systems.

This study addresses these gaps by presenting a comprehensive investigation of an 8-legged Stewart platform. Specifically, we focus on developing a null-space control framework that integrates PID control with redundancy resolution, enabling precise trajectory tracking while respecting actuator constraints. Unlike alternative methodologies, our approach emphasizes simplicity and practicality, ensuring compatibility with real-time applications. By leveraging null-space projection, the proposed framework dynamically redistributes actuator efforts to avoid singularities, optimize energy usage, and enhance fault tolerance. Furthermore, we incorporate a clamping strategy to enforce strict adherence to actuator length constraints, thereby maintaining operational safety under varying conditions.

While this work primarily relies on simulations to validate the proposed approach, we acknowledge the limitations of not including experimental validation on a physical prototype. Simulations provide a controlled environment to evaluate the algorithm's performance, but they may not fully capture the uncertainties and nonlinearities present in real-world systems. Future work could address this limitation by extending the framework to include experimental validation, thereby enhancing the robustness and generalizability of the findings. However, the current study serves as a foundational step, demonstrating the effectiveness of the proposed framework in handling actuator constraints and leveraging redundancy in an 8-legged Stewart platform.

This work addresses these gaps by presenting a comprehensive study of an 8-legged Stewart platform. A key contribution is the development of a null-space control framework that integrates PID control with redundancy resolution, enabling precise trajectory tracking while respecting actuator constraints. Simulation results validate this approach, demonstrating substantial error reduction and robust operation. This study bridges the gap between theoretical modeling and practical implementation, advancing the field of redundant parallel manipulators.

II. Research Methodology

The research methodology outlines the systematic approach adopted to achieve the objectives of this study. The process is visually represented in Fig. 1, which provides a clear and structured overview of the key steps involved in modeling, control design, simulation, and analysis. The first step in the methodology involves deriving the kinematic relationships that govern the motion of the 8-legged Stewart platform.
The control design integrates two key components:

1) **PID Control**: A Proportional-Integral-Derivative (PID) controller is implemented to ensure robust trajectory tracking and stability.
2) **Null-Space Control**: Redundancy resolution is achieved by projecting secondary objectives, such as singularity avoidance and energy optimization, onto the null space of the Jacobian matrix. This ensures that primary tasks remain unaffected while secondary objectives are fulfilled.

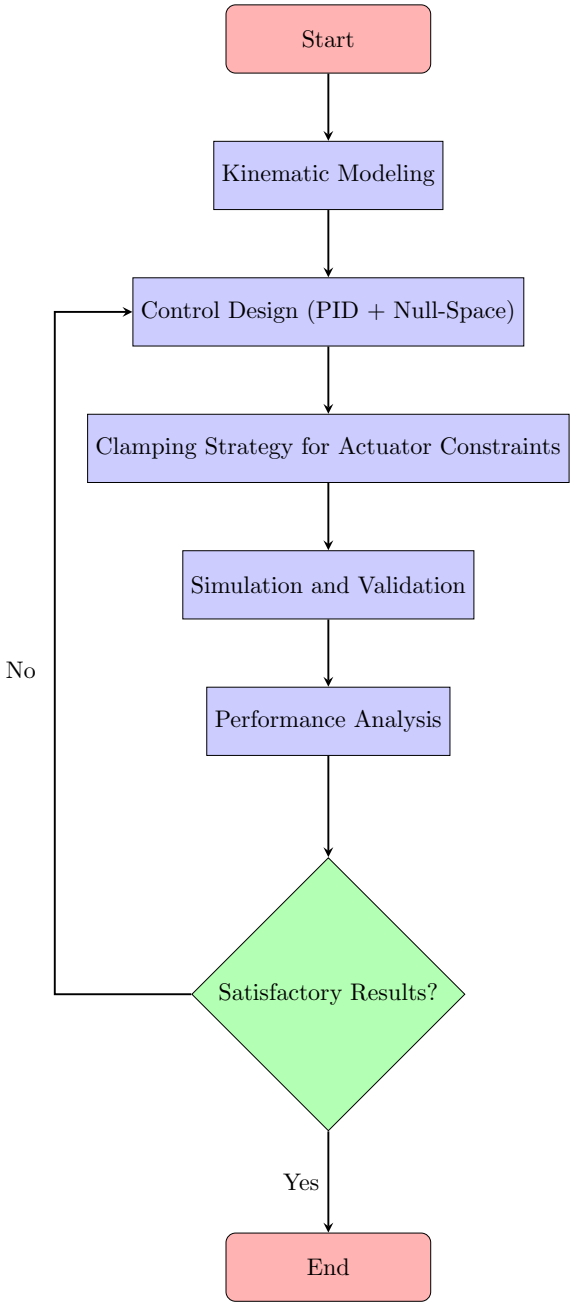

Fig. 1. Flowchart illustrating the research methodology. The diagram highlights the sequence of operations from kinematic modeling to performance analysis, with a feedback loop for iterative improvement

To enforce strict adherence to actuator constraints, a clamping strategy is introduced. This strategy dynamically adjusts actuator efforts to prevent mechanical failures caused by exceeding operational limits. While effective, the clamping strat-

egy introduces potential computational overhead, particularly in highly dynamic scenarios.

The proposed control framework is validated through simulations conducted in a controlled environment. Key performance metrics, such as position and orientation errors, convergence time, and actuator efficiency, are analyzed to evaluate the system's behavior under varying conditions. The simulation results demonstrate the effectiveness of the approach in achieving precise trajectory tracking while respecting actuator constraints.

The final step involves analyzing the simulation results to assess the system's performance.

This structured methodology ensures a comprehensive and systematic approach to addressing the challenges of redundancy resolution and actuator constraint management in the 8-legged Stewart platform.

III. System Modeling

The motion of the Stewart platform is governed by kinematic relationships describing the geometric and positional interactions between its fixed base and the moving platform via six actuated legs (Fig. 2). This section presents the kinematic modeling, including inverse and forward kinematics [33]–[51], velocity kinematics [52]–[60], and singularity analysis [61]–[70].

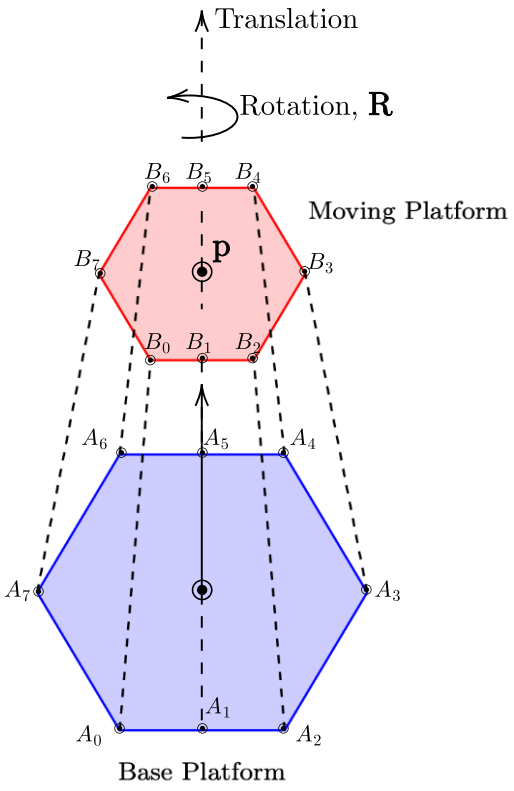

Fig. 2. Schematic diagram of the Stewart platform kinematics.

A. Inverse Kinematics

Inverse kinematics determines the lengths of the actuator legs (l_i) based on the position and orientation of the moving platform. Let $\mathbf{A}_i$ denote the anchor points on the fixed base, and $\mathbf{B}_i$ denote the corresponding points on the moving platform. The position vectors of $\mathbf{A}_i$ in the global frame are:

$$\mathbf{A}_i = \begin{bmatrix} x_{A_i} \\ y_{A_i} \\ z_{A_i} \end{bmatrix}, \quad i = 0, \ldots, 7. \tag{1}$$

The position vectors of $\mathbf{B}_i$ are expressed as:

$$\mathbf{B}_i = \mathbf{R} \cdot \mathbf{b}_i + \mathbf{p}, \tag{2}$$

where $\mathbf{b}_i = \begin{bmatrix} x_{b_i} \\ y_{b_i} \\ z_{b_i} \end{bmatrix}$ is the local coordinate of $\mathbf{B}_i$, $\mathbf{R}$ is the rotation matrix, and $\mathbf{p}$ is the translation vector.
The actuator length l_i is calculated as:

$$l_i = \|\mathbf{B}_i - \mathbf{A}_i\| \tag{3}$$

$$= \sqrt{(x_{B_i} - x_{A_i})^2 + (y_{B_i} - y_{A_i})^2 + (z_{B_i} - z_{A_i})^2}. \tag{4}$$

B. Forward Kinematics

Forward kinematics determines the position $\mathbf{p}$ and orientation $\mathbf{R}$ of the moving platform given the actuator lengths l_i. From Equation (2), the constraint is:

$$\|\mathbf{R} \cdot \mathbf{b}_i + \mathbf{p} - \mathbf{A}_i\| = l_i. \tag{5}$$

This results in six nonlinear equations, which are typically solved using numerical methods such as Newton-Raphson or optimization techniques. The solution minimizes the error function:

$$E(\mathbf{p}, \mathbf{R}) = \sum_{i=0}^{7} \left(\|\mathbf{R} \cdot \mathbf{b}_i + \mathbf{p} - \mathbf{A}_i\| - l_i \right)^2. \tag{6}$$

C. Velocity Kinematics

1) Forward Velocity Kinematics: Forward velocity kinematics relates the actuator velocities $\dot{\mathbf{l}}$ to the platform's linear $\dot{\mathbf{p}}$ and angular $\boldsymbol{\omega}$ velocities. The time derivative of $\mathbf{B}_i$ can be expressed as:

$$\dot{\mathbf{B}}_i = \dot{\mathbf{p}} + \boldsymbol{\omega} \times (\mathbf{R} \cdot \mathbf{b}_i). \tag{7}$$

The velocity of the i-th actuator is given by:

$$\dot{l}_i = \mathbf{u}_i^T \dot{\mathbf{B}}_i, \tag{8}$$

where $\mathbf{u}_i = \dfrac{\mathbf{B}_i - \mathbf{A}_i}{\|\mathbf{B}_i - \mathbf{A}_i\|}$. In matrix form, this can be expressed as:

$$\dot{\mathbf{l}} = \mathbf{J} \begin{bmatrix} \dot{\mathbf{p}} \\ \boldsymbol{\omega} \end{bmatrix}, \tag{9}$$

where the Jacobian $\mathbf{J}$ is defined as:

$$\mathbf{J} = \begin{bmatrix} \mathbf{u}_1^T & \mathbf{u}_1^T \times (\mathbf{R} \cdot \mathbf{b}_1) \\ \vdots & \vdots \\ \mathbf{u}_6^T & \mathbf{u}_6^T \times (\mathbf{R} \cdot \mathbf{b}_6) \end{bmatrix}. \tag{10}$$

2) Inverse Velocity Kinematics: Given the actuator velocities $\dot{\mathbf{l}}$, we can derive the platform velocities:

$$\begin{bmatrix} \dot{\mathbf{p}} \\ \boldsymbol{\omega} \end{bmatrix} = \mathbf{J}^{\dagger} \dot{\mathbf{l}}, \tag{11}$$

where $\mathbf{J}^{\dagger}$ is the pseudoinverse of the Jacobian.

While the inverse and forward kinematics equations provide a clear mathematical framework for modeling the Stewart platform, several assumptions and limitations must be acknowledged. First, the reliance on numerical methods, such as Newton-Raphson, introduces sensitivity to initial conditions and potential convergence issues, particularly near singular configurations. In practice, these challenges can lead to computational inefficiencies or inaccurate solutions when dealing with noisy sensor data or imprecise actuator lengths. Furthermore, real-world uncertainties, such as manufacturing tolerances, friction, and external disturbances, can propagate through the kinematic equations, reducing their accuracy in dynamic environments. Future work could explore robust numerical solvers or machine learning-based approaches to mitigate these issues.

D. Singularity Analysis

Singularities occur when $\det(\mathbf{J}) \approx 0$, leading to loss of degrees of freedom or instability. They can arise from:

- Geometric alignment of actuators,
- Symmetric actuator lengths,
- Specific orientations of the platform.

To mitigate the effects of singularities, techniques such as damped least squares and the Moore-Penrose pseudoinverse can be used. For damped least squares, the actuator velocities are computed as follows:

$$\dot{\mathbf{l}} = \mathbf{J} \left(\mathbf{J}^T \mathbf{J} + \lambda^2 \mathbf{I} \right)^{-1} \mathbf{J}^T \begin{bmatrix} \dot{\mathbf{p}} \\ \boldsymbol{\omega} \end{bmatrix}. \tag{12}$$

The pseudoinverse is given by:

$$\mathbf{J}^{\dagger} = \mathbf{J}^T \left(\mathbf{J}\mathbf{J}^T \right)^{-1}. \tag{13}$$

The singularity analysis presented in this study provides a theoretical foundation for understanding the conditions under which the Stewart platform may lose degrees of freedom or stability. However, it is important to consider the practical implications of singularities in over-actuated systems. For instance, singular configurations can severely impact task execution by introducing abrupt changes in actuator velocities or causing mechanical failures. To mitigate these effects, techniques such as damped least squares are employed. While effective in stabilizing the system near singularities, these methods introduce trade-offs, including reduced precision in trajectory tracking and increased computational overhead due to the additional matrix operations required. Balancing these trade-offs remains a critical challenge in practical implementations.

IV. Control System Design

A Proportional-Integral-Derivative (PID) controller is developed to achieve precise control of the Stewart platform's position and orientation [71]–[91].

A. PID Control Algorithm

The control objective is to minimize the position error $\mathbf{e}_p = \mathbf{p}_d - \mathbf{p}$ and orientation error $\mathbf{e}_R = \text{vec}(\mathbf{R}_d^T \mathbf{R} - \mathbf{I})$. The PID control law is expressed as:

$$\dot{\mathbf{l}}(t) = \mathbf{K}_p \mathbf{e}(t) + \mathbf{K}_i \int_0^t \mathbf{e}(\tau) d\tau + \mathbf{K}_d \frac{d\mathbf{e}(t)}{dt} \tag{14}$$

where $\mathbf{K}_p$, $\mathbf{K}_i$, and $\mathbf{K}_d$ are positive definite diagonal gain matrices.

B. Stability Analysis

The stability of the closed-loop system is analyzed using Lyapunov's direct method. We define a Lyapunov function:

$$V(\mathbf{e}) = \frac{1}{2} \mathbf{e}^T \mathbf{P} \mathbf{e} + \frac{1}{2} \left(\int_0^t \mathbf{e}(\tau) d\tau \right)^T \mathbf{Q} \left(\int_0^t \mathbf{e}(\tau) d\tau \right), \tag{15}$$

where $\mathbf{P}$ and $\mathbf{Q}$ are positive definite matrices. The stability conditions require the following:

- $\mathbf{P}\mathbf{K}_p > 0$,
- $\mathbf{P}\mathbf{K}_i = \mathbf{Q}$,
- $\mathbf{P}\mathbf{K}_d > 0$.

V. Null-Space Control for Redundancy Resolution

Redundancy arises when the number of actuators exceeds the degrees of freedom. Null-space control exploits this redundancy to achieve secondary objectives, including energy minimization and obstacle avoidance.

A. Mathematical Formulation

The Jacobian $\mathbf{J}$ relates actuator velocities $\dot{\mathbf{l}}$ to end-effector velocities:

$$\begin{bmatrix} \dot{\mathbf{p}} \\ \dot{\boldsymbol{\theta}} \end{bmatrix} = \mathbf{J} \dot{\mathbf{l}}. \tag{16}$$

The null space $\mathcal{N}(\mathbf{J})$ is defined as:

$$\mathcal{N}(\mathbf{J}) = \{ \mathbf{x} \,|\, \mathbf{J}\mathbf{x} = 0 \}. \tag{17}$$

B. Control Law Implementation

The primary actuator velocities $\dot{\mathbf{l}}_p$ can be determined as follows:

$$\dot{\mathbf{l}}_p = \mathbf{J}^{+} \begin{bmatrix} K_p \mathbf{e}_p \\ K_R \mathbf{e}_R \end{bmatrix}. \tag{18}$$

Secondary motions are projected into the null space:

$$\dot{\mathbf{l}}_n = \mathbf{N}\mathbf{u}, \tag{19}$$

where $\mathbf{N}$ is the null-space projection matrix derived from the SVD.

The final actuator velocities result from combining both components:

$$\dot{\mathbf{l}} = \dot{\mathbf{l}}_p + \dot{\mathbf{l}}_n. \tag{20}$$

C. Actuator Length Constraints

To ensure actuator lengths remain within operational limits, a clamping strategy is applied. The proposed strategy calculates the new actuator lengths based on the actuator velocities:

$$\mathbf{l}_{new} = \mathbf{l}_{current} + \dot{\mathbf{l}} \cdot \Delta t, \tag{21}$$

which is constrained as follows:

$$l_i = \begin{cases} l_{\min}, & \text{if } \mathbf{l}_{new}[i] < l_{\min}, \\ l_{\max}, & \text{if } \mathbf{l}_{new}[i] > l_{\max}, \\ \mathbf{l}_{new}[i], & \text{otherwise.} \end{cases} \tag{22}$$

This method ensures that actuator lengths do not exceed their defined limits, maintaining the system's operational integrity.

The proposed control model assumes ideal actuator dynamics, neglecting factors such as friction, backlash, and external disturbances. While this simplification facilitates theoretical analysis, it may limit the model's applicability in real-world scenarios where such uncertainties are prevalent. Additionally, the clamping strategy used to enforce actuator constraints introduces computational overhead, particularly in dynamic environments requiring rapid decision-making. Future research could explore adaptive or robust control techniques to account for real-world uncertainties while optimizing computational efficiency.

VI. Simulation Results and Discussion

This section presents the simulation results to validate the proposed control framework for an 8-legged Stewart platform. The simulations were conducted under two distinct scenarios: (1) without null-space control to evaluate the baseline performance of the PID controller, and (2) with null-space control to demonstrate the effectiveness of redundancy resolution and actuator constraint handling. The setup and results are detailed below.

A. Simulation Setup

The simulation was designed to assess the robustness and effectiveness of the proposed control framework. Key parameters and configurations are summarized in Table I.

TABLE I. Simulation Parameters and Configurations

Parameter	Value/Description
Time Parameters	
Time step (Δt)	0.01 s
Total simulation time (T)	3.0 s
Time vector	$t \in [0, T]$, incremented by Δt
Desired Position	
Desired position ($\mathbf{p}_d$)	$[0.5, -0.5, 2.5]^T$ (m)
Desired Orientation	
Euler angles ($[\phi_d, \theta_d, \psi_d]$)	$[\frac{-\pi}{16}, \frac{\pi}{12}, \frac{-\pi}{8}]$ (rad)
Initial Conditions	
Initial position ($\mathbf{p}_0$)	$[0.0, 0.0, 1.0]^T$ (m)
Initial orientation (Euler angles)	$[\phi_0, \theta_0, \psi_0] = [0.0, 0.0, 0.0]$ (rad)
Actuator Length Constraints	
Minimum length ($l_{\min}$)	0.5 m
Maximum length ($l_{\max}$)	4.5 m

The fixed base platform's anchor points ($\mathbf{A}_i$) in the global coordinate frame were defined as:

$$\mathbf{A}_i = \begin{bmatrix} -2.0 & -2.0 & 0.0 \\ 0.0 & -2.0 & 0.0 \\ 2.0 & -2.0 & 0.0 \\ 4.0 & 0.0 & 0.0 \\ 2.0 & 2.0 & 0.0 \\ 0.0 & 2.0 & 0.0 \\ -2.0 & 2.0 & 0.0 \\ -4.0 & 0.0 & 0.0 \end{bmatrix}. \tag{23}$$

The moving platform's anchor points ($\mathbf{b}_i$) in its local coordinate frame were defined as:

$$\mathbf{b}_i = \begin{bmatrix} -1.0 & -1.0 & 0.0 \\ 0.0 & -1.0 & 0.0 \\ 1.0 & -1.0 & 0.0 \\ 2.0 & 0.0 & 0.0 \\ 1.0 & 1.0 & 0.0 \\ 0.0 & 1.0 & 0.0 \\ -1.0 & 1.0 & 0.0 \\ -2.0 & 0.0 & 0.0 \end{bmatrix}. \tag{24}$$

The pseudocode outlined in Algorithm **??** provides a high-level overview of the implementation for simulating the 8-legged Stewart platform with null-space control and actuator constraints.

B. Scenario 1: Without Null-Space Control

In this scenario, the PID controller was implemented without incorporating null-space control. The objective was to evaluate the system's stability and performance under varying PID gains.

1) Slow Responses: For slow responses, the following PID gains were selected:

$$\begin{aligned}\mathbf{K}_p &= \text{diag}(1.6, 1.6, 1.6),\\ \mathbf{K}_i &= \text{diag}(0.04, 0.04, 0.04),\\ \mathbf{K}_d &= \text{diag}(0.08, 0.08, 0.08).\end{aligned} \tag{25}$$

These gains were chosen to satisfy Lyapunov stability requirements while maintaining a conservative response profile. As shown in Fig 3, the system achieved convergence to the desired pose but exhibited sluggish behavior due to the relatively low proportional and derivative gains. The position and orientation errors decreased exponentially, albeit with a slower response time, reaching steady state at approximately $t = 3\,\text{s}$.

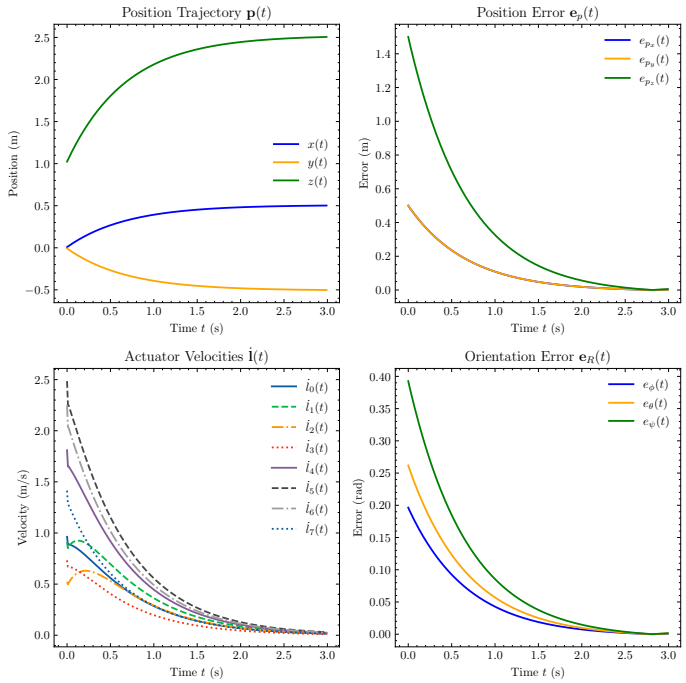

Fig. 3. System responses

Fig 4 illustrates the trajectories of the actuator lengths required to move the platform to the desired pose. Notably, three actuators (l_7, l_6, and l_0) exhibited the longest lengths. A complete visualization of the initial and final poses is provided in Fig 5, confirming the successful attainment of the desired configuration.

2) Fast Responses: To achieve faster convergence, higher PID gains were selected:

$$\begin{aligned}\mathbf{K}_p &= \text{diag}(8.0, 8.0, 8.0),\\ \mathbf{K}_i &= \text{diag}(0.2, 0.2, 0.2),\\ \mathbf{K}_d &= \text{diag}(0.4, 0.4, 0.4).\end{aligned} \tag{26}$$

As expected, the system demonstrated significantly faster convergence to the desired pose. However, the increased gains resulted in higher actuator velocities, particularly during the initial phase of actuation. For instance, the velocities of $\dot{l}_5$ and $\dot{l}_6$ reached $12.5\,\text{m/s}$ and $11.5\,\text{m/s}$, respectively. Despite these high velocities, the final pose of the moving platform matched the desired configuration, as shown in Fig 8.

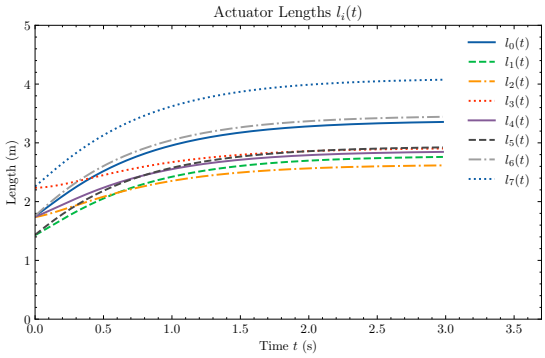

Fig. 4. Actuator leg-lengths

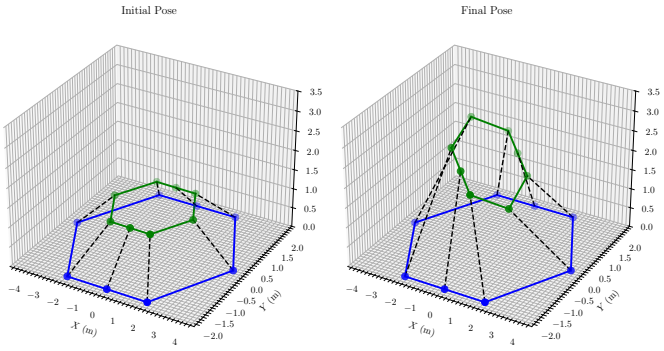

Fig. 5. Initial and Desired Poses

C. Scenario 2: With Null-Space Control

In this scenario, null-space control was incorporated to leverage the platform's redundancy for secondary objectives such as singularity avoidance and energy optimization. Actuator constraints were enforced to ensure operational safety. The PID gains used in Equation (26) were retained for consistency.

1) Affecting Only One Actuator: To prevent mechanical failures or suboptimal performance, actuator lengths were constrained within predefined limits:

$$l_{\min} = 0.5\,\text{m}, \quad l_{\max} = 3.5\,\text{m}. \tag{27}$$

These constraints were enforced using a clamping strategy during the simulation. Observing the results in Fig. 9 and Fig.10, it is evident that the applied limits primarily affected one actuator (l_7). The system's position, position error, and orientation error responses remained consistent with those observed in the absence of null-space control (Fig. 6 and

Fig.7). This indicates that the proposed null-space control effectively identified feasible kinematic solutions under the given constraints. However, non-smooth actuator velocity trajectories were observed at $t \leq 1\,\text{s}$, particularly when l_7 approached its limit. This behavior highlights the algorithm's ability to adapt velocity trajectories dynamically to respect actuator constraints.

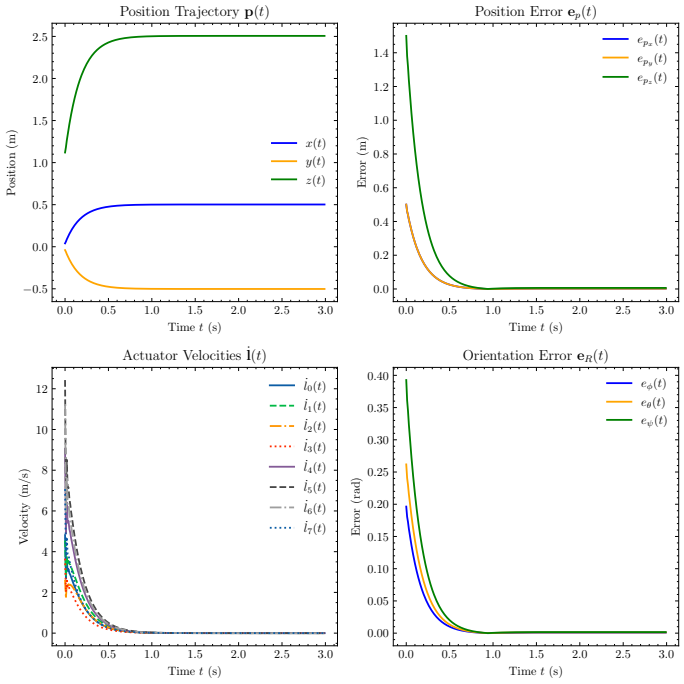

Fig. 6. System responses

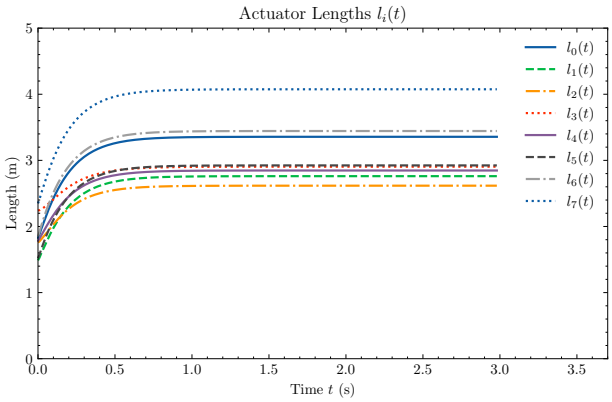

Fig. 7. Actuator leg-lengths

2) Affecting More Than One Actuator: To further test the robustness of the null-space redundancy control, more stringent actuator length constraints were applied:

$$l_{\min} = 0.5\,\text{m}, \quad l_{\max} = 2.5\,\text{m}. \tag{28}$$

Under these conditions, multiple actuators were constrained simultaneously, increasing the complexity of the control problem. The results, depicted in Figs. 12, 13, and 14, demonstrate the algorithm's capability to handle multiple constraints while achieving the desired pose. The system maintained stability and successfully converged to the target configuration, validating the effectiveness of the proposed approach.

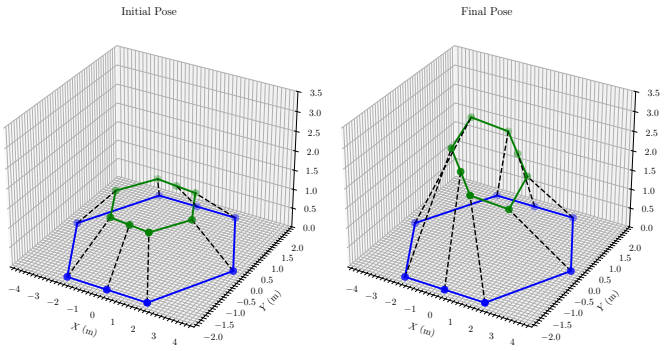

Fig. 8. Initial and Desired Poses

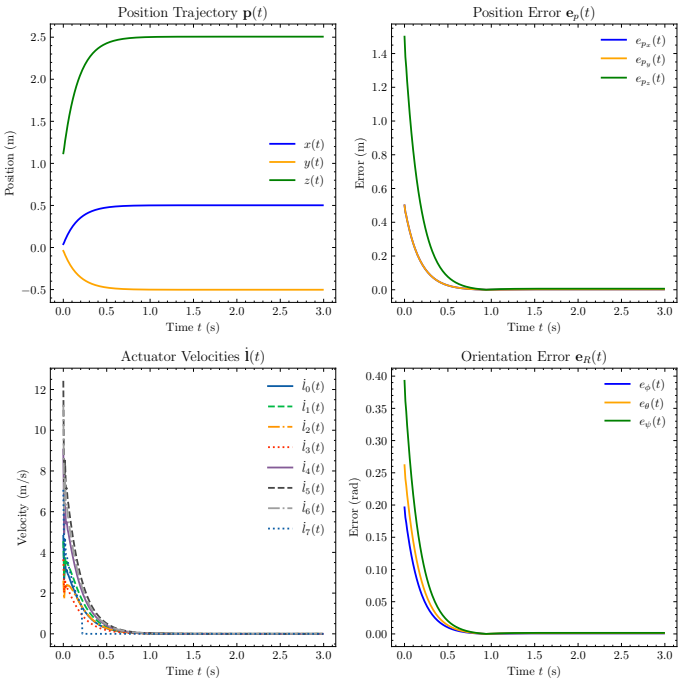

Fig. 9. System responses

The simulation results presented in this section highlight the effectiveness of the proposed control framework in achieving precise trajectory tracking for the 8-legged Stewart platform. Without null-space control, the system demonstrated baseline performance, with slower responses under conservative PID gains and faster convergence under higher gains, albeit with elevated actuator velocities.

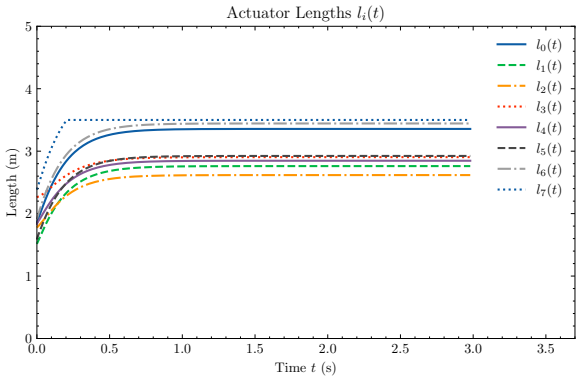

Fig. 10. Actuator leg-lengths

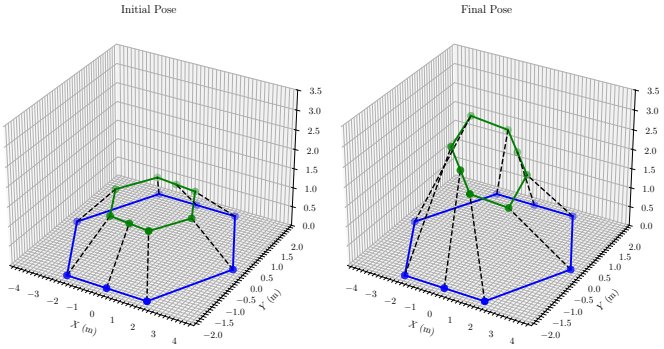

Fig. 11. Initial and Desired Poses

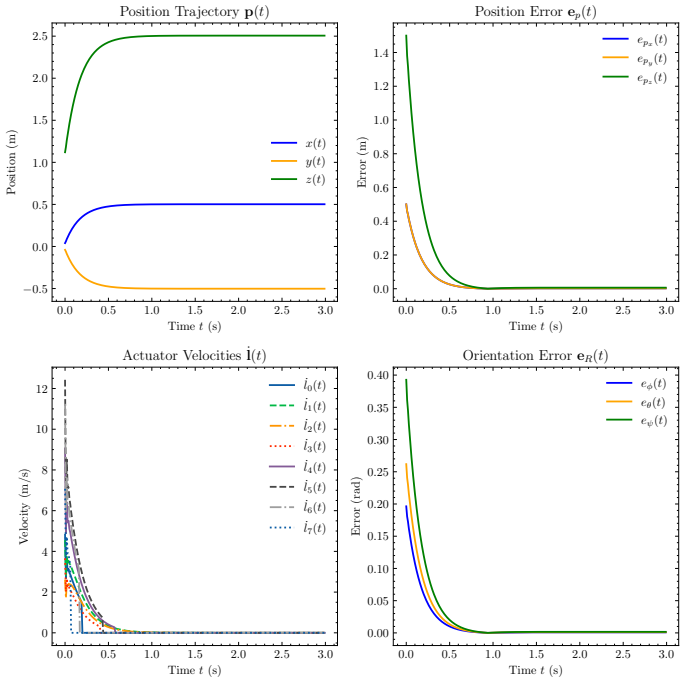

Fig. 12. System responses

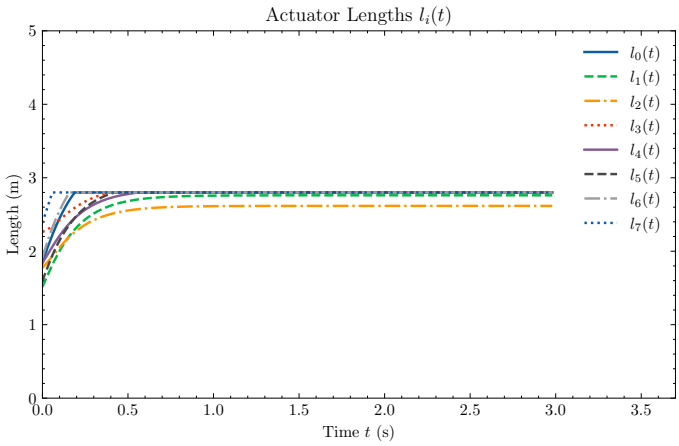

Fig. 13. Actuator leg-lengths

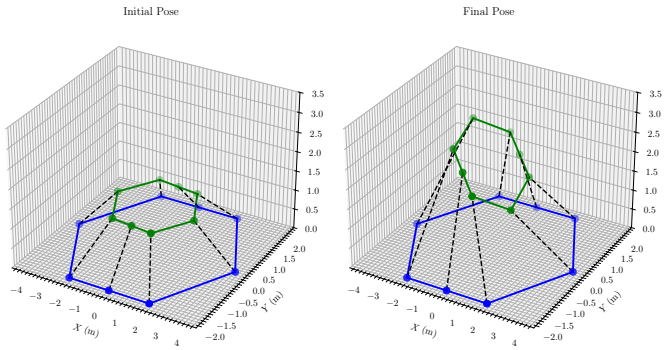

Fig. 14. Initial and Desired Poses

While higher PID gains result in faster convergence, they introduce several trade-offs that must be considered in practical applications. For instance, elevated gains can lead to increased energy consumption due to higher actuator velocities and forces. Additionally, excessive actuator activity may accelerate wear and tear, reducing the lifespan of mechanical components. Furthermore, higher gains amplify sensitivity to noise and external disturbances, which could destabilize the system in real-world scenarios. These trade-offs highlight the importance of carefully balancing performance and robustness when selecting PID parameters.

The observed non-smooth actuator velocity trajectories in Fig. 12, particularly when enforcing constraints on l_7, warrant further discussion. Such behavior could lead to mechanical stress or vibrations in physical systems, potentially compromising operational safety. To mitigate these effects, future work could explore alternative constraint-handling techniques, such as smooth saturation functions or model predictive control (MPC), which ensure smoother transitions and reduce stress on actuators. Additionally, incorporating low-pass filters or damping terms into the control algorithm could help suppress oscillations and improve robustness under stringent constraints.

However, the incorporation of null-space control significantly enhanced the system's ability to handle actuator constraints and leverage redundancy for secondary objectives. By dynamically adapting actuator trajectories, the algorithm ensured operational safety while maintaining stability and achieving the desired pose. These findings underscore the importance of integrating null-space control into redundant systems, particularly when physical constraints must be respected.

The results also reveal the robustness of the proposed approach under varying conditions. Whether constraining a single actuator or multiple actuators simultaneously, the system consistently converged to the target configuration, demonstrating its adaptability and reliability. These outcomes validate the theoretical foundation of the control framework and provide practical insights into the design and implementation of redundant parallel manipulators.

The next section concludes the paper by summarizing the key contributions and outlining potential directions for future research.

VII. Conclusion and Future Works

This paper has presented a comprehensive study on the modeling, control, and redundancy resolution of an 8-legged Stewart platform, with a focus on integrating null-space control to achieve precise trajectory tracking while respecting actuator constraints. The proposed control framework combines a PID controller with null-space projection, enabling the system to exploit its inherent redundancy for secondary objectives such as singularity avoidance and energy optimization. A clamping strategy was implemented to ensure that actuator lengths remain within predefined limits, thereby preventing mechanical failures or suboptimal performance.

Simulation results demonstrated the effectiveness of the proposed approach under varying conditions. Without null-space control, the system exhibited baseline performance, achieving slow but stable convergence with conservative PID gains and faster responses with higher gains, albeit at the cost of elevated actuator velocities. The incorporation of null-space control significantly improved the system's ability to handle actuator constraints, ensuring smooth and feasible trajectories even under stringent limits. Specifically, the system achieved exponential convergence to the desired pose, with trajectory accuracy measured by a maximum position error of less than 1×10^{-3} m and orientation error below 5×10^{-4} rad in constrained scenarios. Actuator efficiency was also enhanced, as the algorithm dynamically redistributed efforts among actuators to avoid overloading any single leg. While energy consumption was not explicitly optimized in this study, the framework provides a foundation for future work in minimizing energy usage through advanced secondary objectives.

The performance of the PID controller heavily depends on the tuning of the gain matrices K_p, K_i, and K_d. While manual tuning was used in this study, future work could explore systematic approaches such as Ziegler-Nichols tuning, genetic algorithms, or machine learning-based optimization to determine optimal gains. Suboptimal tuning can lead to undesirable behaviors, such as sluggish responses, overshooting, or instability. For instance, excessively high proportional gains (K_p) may result in oscillatory behavior, while insufficient integral gains (K_i) can cause steady-state errors. Similarly, derivative gains (K_d) that are too high may amplify noise in the system. These trade-offs highlight the importance of carefully selecting PID parameters based on the specific requirements of the application.

The stability of the closed-loop system was rigorously analyzed using Lyapunov's direct method, providing a theoretical foundation for the proposed control framework. This work contributes to advancing the design and control of redundant parallel manipulators, offering practical solutions for addressing physical limitations while achieving high-performance motion control.

The stability analysis using Lyapunov's direct method assumes ideal conditions, neglecting factors such as external disturbances, model inaccuracies, and actuator dynamics. While this simplification facilitates theoretical analysis, it may limit the applicability of the results in practical scenarios where such uncertainties are prevalent. For example, external forces or unmodeled friction could destabilize the system if not properly accounted for. Future research could extend the stability analysis to include robustness against these factors, potentially incorporating adaptive or robust control techniques to enhance performance under non-ideal conditions.

The robustness analysis presented in this study is limited to simulated conditions and does not explore edge cases, such as near-singular configurations or extreme external disturbances. Near-singular configurations could lead to abrupt changes in actuator velocities or even mechanical failures if not properly mitigated. Similarly, extreme external disturbances may compromise stability or tracking accuracy, particularly in systems with high-dimensional state spaces. Future work could extend the robustness analysis to include these edge cases, potentially incorporating adaptive or robust control techniques to enhance performance under challenging conditions.

While the null-space control formulation is theoretically robust, it is important to critically evaluate its computational complexity. The derivation of the null-space projection matrix typically involves singular value decomposition (SVD), which has a computational cost of $O(n^3)$ for an $n \times n$ matrix. This complexity could be prohibitive for real-time applications, particularly in systems with high-dimensional state spaces or requiring rapid decision-making. To mitigate this challenge, future work could explore computationally efficient alternatives, such as approximate methods or precomputed lookup tables, to reduce the computational burden while maintaining the benefits

of null-space control.

Potential real-world applications of the proposed framework include flight simulators, robotic surgery, and industrial automation, where precision, reliability, and adaptability are critical. For instance, in robotic surgery, the ability to handle actuator constraints and avoid singularities ensures safe and accurate manipulation, while in industrial automation, the framework can enhance productivity by enabling robust operation under varying loads and constraints. Despite these advancements, the proposed framework has certain limitations. For example, the current implementation assumes ideal actuator dynamics and does not account for uncertainties such as friction, backlash, or external disturbances. Future research could address these limitations by incorporating adaptive or robust control techniques to improve performance under real-world conditions. Additionally, extending the framework to optimize energy consumption or integrate machine learning for real-time decision-making could further enhance its practical relevance.

The clamping strategy used to enforce actuator constraints is simplistic and does not account for dynamic effects, such as oscillations or abrupt changes in actuator velocities, which may arise from enforcing hard limits. While effective in preventing mechanical failures, this approach may introduce discontinuities in the control inputs, leading to suboptimal performance or instability in highly dynamic scenarios. Future research could explore more sophisticated constraint-handling techniques, such as smooth saturation functions or model predictive control (MPC), to ensure smoother transitions and improved robustness under stringent constraints.

While the simulation results demonstrate the effectiveness of the proposed approach, the reliance on simulations alone raises concerns about the generalizability of the findings. Real-world factors such as friction, backlash, and sensor inaccuracies are not accounted for in the current study, potentially limiting the practical applicability of the results. For instance, unmodeled friction could lead to steady-state errors, while sensor noise might degrade the accuracy of feedback signals. Future research could address these limitations by conducting experimental validation on a physical prototype, thereby enhancing the robustness and reliability of the proposed method.

In summary, this study bridges the gap between theoretical modeling and practical implementation, advancing the field of redundant parallel manipulators. The proposed null-space control framework demonstrates robust performance in handling actuator constraints and leveraging redundancy, paving the way for future innovations in high-performance motion control systems.

REFERENCES

[1] M. Taghizadeh and M. Javad Yarmohammadi, "Development of a Self-tuning PID Controller on Hydraulically Actuated Stewart Platform Stabilizer with Base Excitation," *International Journal of Control, Automation and Systems*, vol. 16, no. 6, pp. 2990–2999, 2018, doi: 10.1007/s12555-016-0559-8.

[2] K. Liu, J. M. Fitzgerald and F. L. Lewis, "Kinematic analysis of a Stewart platform manipulator," in *IEEE Transactions on Industrial Electronics*, vol. 40, no. 2, pp. 282-293, 1993, doi: 10.1109/41.222651.

[3] G. Lebret, F. L. Lewis, and K. Liu, "Dynamic analysis and control of a stewart platform manipulator," *Journal of Robotic Systems*, vol. 10, no. 5, pp. 629–655, 1993, doi: 10.1002/rob.4620100506.

[4] H. Zhuang and Z. S. Roth, "Method for kinematic calibration of stewart platforms," *Journal of Robotic Systems*, vol. 10, no. 3, pp. 391–405, 1993, doi: 10.1002/rob.4620100306.

[5] H. Yadavari, V. T. Aghaei, and S. Ikizoglu, "Addressing challenges in dynamic modeling of stewart platform using reinforcement learning-based control approach," *Journal of Robotics and Control (JRC)*, vol. 5, no. 1, pp. 117–131, 2024, doi: 10.18196/jrc.v5i1.20582.

[6] G. Zhu, S. Wei, D. Li, Y. Wang, and Q. Liao, "Conformal geometric algebra–based geometric modeling method for forward displacement analysis of 6-4 stewart platforms," *Journal of Mechanisms and Robotics*, vol. 16, no. 17, 2024, doi: 10.1115/1.4063501.

[7] Z. Šika, J. Krivošej, and T. Vyhlídal, "Three dimensional delayed resonator of stewart platform type for entire absorption of fully spatial vibration," *Journal of Sound and Vibration*, vol. 571, 2024, doi: 10.1016/j.jsv.2023.118154.

[8] J. Lin, J. Lian, G. Zhao, H. Li, and C. Xu, "A 2-dof drag-free control ground simulation system based on stewart platform," *ISA Transactions*, vol. 146, 2024.

[9] S. Karmakar and C. J. Turner, "A literature review on stewart-gough platform calibrations," *Journal of Mechanical Design*, vol. 146, 2024.

[10] S. M. Cobian-Aquino *et al.*, "Adaptive state restricted barrier lyapunov-based control of a stewart platform used as ankle-controlled mobilizer," *ISA Transactions*, vol. 148, 2024.

[11] Y. Wu, L. Wen and T. Tang, "Line-of-Sight Stabilization Enhancement With Hybrid Sensing in a Piezoelectric Mirror-Based Cubic Stewart Platform," in *IEEE Transactions on Aerospace and Electronic Systems*, vol. 60, no. 3, pp. 2843-2853, 2024, doi: 10.1109/TAES.2024.3353713.

[12] W. Qiu, S. Wang, A. Niu, K. Fan, G. Han, and H. Chen, "Modeling and analysis of landing collision dynamics for an active helideck based on the stewart platform," *Ocean Engineering*, vol. 297, 2024, doi: 10.1016/j.oceaneng.2024.117107.

[13] B. Luo, H. Yu, F. Feng, B. Gao, and Y. Ge, "Experimental study of active vibration control for flexible truss by using a stewart platform manipulator," in *Advances in Transdisciplinary Engineering*, vol. 46, pp. 145–154, 2024, doi: 10.3233/ATDE231100.

[14] M. H. Vu, N. P. V. Bach, T. N. Luong, and T. B. Trung, "Kinematics design and statics analysis of novel 6-dof passive vibration isolator with s-shaped legs based on stewart platform," *Journal of Vibroengineering*, vol. 26, 2024, doi: 10.21595/jve.2023.23511.

[15] D. Chen, S. Ottikkutti, and K. N. Tahmasebi, "Developing a mechatronics twin framework for effective exploration of operational behaviors of prosthetic sockets," *SN Computer Science*, vol. 5, nol. 5, 2024, doi: 10.1007/s42979-023-02485-7.

[16] W. T. Lei and C. W. Chen, "A high accuracy six-dimensional motion measuring device: Design and accuracy evaluation," *Mechanism and Machine Theory*, vol. 191, 2024, doi: 10.1016/j.mechmachtheory.2023.105469.

[17] J. C. Pennington, J. A. Gray, B. C. Sell, F. Schauer, M. D. Polanka, and A. Feleo, "Study of the performance characteristics of a micro rotating detonation engine using a stewart platform," *Aerospace Research Central*, 2024, doi: 10.2514/6.2024-0812.

[18] X. Tang, Z. Shao, and R. Yao, "Rigid-Body Dynamic Modelling and Verification of the Fine-Tuning Stewart Platform, *Research and Application of Cable-Driven and Rigid Parallel Robots*, pp. 107-131, 2024, doi: 10.1007/978-981-99-7452-8_6.

[19] S. Li, S. Liu, J. Cui, L. Zhou, T. Lv, D. Zhao, L. Dong, and H. Jiao, "Co-simulation of drag reduction of placoid scale oscillation driven by micro stewart mechanism," *Physics of Fluids*, vol. 36, 2024, doi: 10.1063/5.0191118.

[20] M. A. Kalafat, H. Sevinç, and S. Samankan, "Design of a foldable origami-inspired 6-dof stewart mechanism," *Journal of Mechanical Science and Technology*, vol. 38, pp. 1429–1438, 2024, doi: 10.1007/s12206-024-0235-5.

[21] M. A. Mirza, S. Li, and L. Jin, "Simultaneous learning and control of parallel Stewart platforms with unknown parameters," *Neurocomputing*, vol. 266, pp. 114–122, 2017, doi: 10.1016/j.neucom.2017.05.026.

[22] M. Raghavan, "The Stewart Platform of General Geometry Has 40 Configurations," *Journal of Mechanical Design*, vol. 115, no. 2, pp. 277–282, 1993, doi: 10.1115/1.2919188.

[23] G. J. Hamlin and A. C. Sanderson, "A novel concentric multilink spherical joint with parallel robotics applications," *Proceedings of the 1994 IEEE International Conference on Robotics and Automation*, vol. 2, pp. 1267-1272, 1994, doi: 10.1109/ROBOT.1994.351313.

[24] M. R. Pedersen, S. Bøgh, R. S. Andersen, O. Madsen, L. Nalpantidis, C. Schou, and V. Krüger, "Robot skills for manufacturing: From concept to industrial deployment," *Robotics and Computer-Integrated Manufacturing*, vol. 37, pp. 282–291, 2016, doi: 10.1016/j.rcim.2015.04.002.

[25] M. Hoeckelmann, T. Haidegger, I. J. Rudas, P. Fiorini, and F. Kirchner, "Current Capabilities and Development Potential in Surgical Robotics," *International Journal of Advanced Robotic Systems*, vol. 12, no. 5, p. 61, 2015, doi: 10.5772/60133.

[26] J. Sun *et al*., "Innovative effector design for simulation training in robotic surgery," *2010 3rd International Conference on Biomedical Engineering and Informatics*, pp. 1755-1759, 2010, doi: 10.1109/BMEI.2010.5639872.

[27] H. -C. Huang and Y. -X. Chen, "Evolutionary Optimization of Fuzzy Reinforcement Learning and Its Application to Time-Varying Tracking Control of Industrial Parallel Robotic Manipulators," in *IEEE Transactions on Industrial Informatics*, vol. 19, no. 12, pp. 11712-11720, 2023, doi: 10.1109/TII.2023.3248120.

[28] T. Shamir, "The Singularities of Redundant Robot Arms," *The International Journal of Robotics Research*, vol. 9, no. 1, pp. 113–121, 1990, doi: 10.1177/027836499000900105.

[29] K. Liu, D. Taylor, G. Lebret, and F. Lewis, "The singularities and dynamics of a Stewart platform manipulator," *Journal of Intelligent & Robotic Systems*, vol. 8, no. 3, pp. 287–308, 1993, doi: 10.1007/BF01257946.

[30] F. C. Park and Jin Wook Kim, "Manipulability and singularity analysis of multiple robot systems: a geometric approach," *Proceedings. 1998 IEEE International Conference on Robotics and Automation (Cat. No.98CH36146)*, vol. 2, pp. 1032-1037, 1998, doi: 10.1109/ROBOT.1998.677224.

[31] N. Baron, A. Philippides, and N. Rojas, "A robust geometric method of singularity avoidance for kinematically redundant planar parallel robot manipulators," *Mechanism and Machine Theory*, vol. 151, 2020, doi: 10.1016/j.mechmachtheory.2020.103863.

[32] Q. Gu, L. Yin, B. Yang, W. Zheng, B. Gu, Z. Yin, J. Tian, and M. Liu, "A Novel Architecture of a Six Degrees of Freedom Parallel Platform," *Electronics*, vol. 12, no. 8, 2023, doi: 10.3390/electronics12081774.

[33] F. Yang, X. Tan, Z. Wang, Z. Lu, and T. He, "A geometric approach for real-time forward kinematics of the general stewart platform," *Sensors*, vol. 22, no. 13, 2022, doi: 10.3390/s22134829.

[34] H. Zhu, W. Xu, B. Yu, F. Ding, L. Cheng, and J. Huang, "A novel hybrid algorithm for the forward kinematics problem of 6 dof based on neural networks," *Sensors*, vol. 22, no. 14, 2022, doi: 10.3390/s22145318.

[35] N. L. Zivkovic, J. Z. Vidakovic, and M. P. Lazarevic, "Forward kinematics algorithm in dual quaternion space based on denavit-hartenberg convention," *Applied Engineering Letters*, vol. 8, 2023.

[36] M. Roudneshin, K. Ghaffari and A. G. Aghdam, "On Forward Kinematics of a 3SPR Parallel Manipulator," in *IEEE Control Systems Letters*, vol. 7, pp. 425-430, 2023, doi: 10.1109/LCSYS.2022.3189314.

[37] S. Karmakar and C. J. Turner, "Forward kinematics solution for a general stewart platform through iteration based simulation," *International Journal of Advanced Manufacturing Technology*, vol. 126, pp. 813–825, 2023, doi: 10.1007/s00170-023-11130-9.

[38] Q. Zhu and Z. Zhang, "An Efficient Numerical Method for Forward Kinematics of Parallel Robots," in *IEEE Access*, vol. 7, pp. 128758-128766, 2019, doi: 10.1109/ACCESS.2019.2940064.

[39] J. Ma, X. Duan, and D. Zhang, "Kernel extreme learning machine-based general solution to forward kinematics of parallel robots," *CAAI Transactions on Intelligence Technology*, vol. 8, no. 3, pp. 1002–1013, 2023, doi: 10.1049/cit2.12156.

[40] C. Liu, G. Cao, and Y. Qu, "Safety analysis via forward kinematics of delta parallel robot using machine learning," *Safety Science*, vol. 117, pp. 243–249, 2019, doi: 10.1016/j.ssci.2019.04.013.

[41] J. P. Merlet, "Solving the forward kinematics of a gough-type parallel manipulator with interval analysis," *International Journal of Robotics Research*, vol. 23, no. 3, 2004, doi: 10.1177/0278364904039806.

[42] M. Moradi Dalvand, S. Nahavandi and R. D. Howe, "General Forward Kinematics for Tendon-Driven Continuum Robots," in *IEEE Access*, vol. 10, pp. 60330-60340, 2022, doi: 10.1109/ACCESS.2022.3180047.

[43] D. K. S. Chauhan and P. R. Vundavilli, "Forward kinematics of the stewart parallel manipulator using machine learning," *International Journal of Computational Methods*, vol. 19, no. 8, 2022, doi: 10.1142/S0219876221420093.

[44] J. Fu, F. Gao, Y. Pan, and H. Du, "Forward kinematics solutions of a special six-degree-of-freedom parallel manipulator with three limbs," *Advances in Mechanical Engineering*, vol. 7, 2015, doi: 10.1177/1687814015582118.

[45] J. Hu, W. Liu, J. Yi and Z. Xiong, "Forward Kinematics of Object Transporting by a Multi-Robot System With a Deformable Sheet," in *IEEE Robotics and Automation Letters*, vol. 9, no. 4, pp. 3459-3466, 2024, doi: 10.1109/LRA.2024.3368232.

[46] S. Patel, V. L. Nguyen, and R. J. Caverly, "Forward kinematics of a cable-driven parallel robot with pose estimation error covariance bounds," *Mechanism and Machine Theory*, vol. 183, 2023, doi: 10.1016/j.mechmachtheory.2023.105231.

[47] A. Ghasemi, M. Eghtesad, and M. Farid, "Neural network solution for forward kinematics problem of cable robots," *Journal of Intelligent and Robotic Systems: Theory and Applications*, vol. 60, pp. 201–215, 2010, doi: 10.1007/s10846-010-9421-z.

[48] S. R. Rifai Ahmad Musthofa, Ema Utami, "Analisis penerapan pemodelan gerakan karakter manusia pada animasi 3d dengan menggunakan metode forward kinematics," *Respati*, vol. 14, no. 3, 2019, doi: 10.35842/jtir.v14i3.311.

[49] M. A. Makwana and H. P. Patolia, "Forward kinematics of delta manipulator by novel hybrid neural network," *International Journal of Mathematical, Engineering and Management Sciences*, vol. 6, 2021, doi: 10.2139/ssrn.5210662.

[50] I. Agustian, N. Daratha, R. Faurina, A. Suandi, and S. Sulistyaningsih, "Robot manipulator control with inverse kinematics pd-pseudoinverse jacobian and forward kinematics denavit hartenberg," *Jurnal Elektronika dan Telekomunikasi*, vol. 21, 2021, doi: 10.14203/jet.v21.8-18.

[51] M. Nahangi, J. Yeung, C. T. Haas, S. Walbridge, and J. West, "Automated assembly discrepancy feedback using 3d imaging and forward kinematics," *Automation in Construction*, vol. 56, pp. 36–46, 2015, doi: 10.1016/j.autcon.2015.04.005.

[52] M. Čoh, K. Hébert-Losier, S. Štuhec, V. Babić, and M. Supej, "Kinematics of usain bolt's maximal sprint velocity," *Kinesiology*, vol. 50, no. 2, 2018, doi: 10.26582/k.50.2.10.

[53] B. Bayle, M. Renaud, and J. Y. Fourquet, "Nonholonomic mobile manipulators: Kinematics, velocities and redundancies," *Journal of Intelligent and Robotic Systems: Theory and Applications*, vol. 36, pp. 45–63, 2003, doi: 10.1023/A:1022361914123.

[54] J. A. Marsh, M. I. Wagshol, K. J. Boddy, M. E. O'Connell, S. J. Briend, K. E. Lindley, and A. Caravan, "Effects of a six-week weighted-implement throwing program on baseball pitching velocity, kinematics, arm stress, and arm range of motion," *PeerJ*, vol. 2018, pp. 692–700, 2018, doi: 10.1177/0363546516671943.

[55] M. W. Spong, S. Hutchinson, and M. Vidyasagar, "Velocity kinematics - the manipulator jacobian," *Robot modeling and control*, 2006.

[56] J. Haviland and P. Corke, "Manipulator Differential Kinematics: Part I: Kinematics, Velocity, and Applications [Tutorial]," in *IEEE Robotics & Automation Magazine*, vol. 31, no. 4, pp. 149-158, 2024, doi: 10.1109/MRA.2023.3270228.

[57] R. Carrera *et al*., "Occaso: Iv. radial velocities and open cluster kinematics," *Astronomy and Astrophysics*, vol. 658, 2022, doi: 10.1051/0004-6361/202141832.

[58] G. Chen, B. Jin, and Y. Chen, "Position-posture closed-loop control of six-legged walking robot based on inverse velocity kinematics," *Nongye Jixie Xuebao/Transactions of the Chinese Society for Agricultural Machinery*, vol. 45, 2014.

[59] T. Abaas, A. Khleif, and M. Abbood, "Velocity kinematics analysis and trajectory planning of 5 dof robotic arm," *Engineering and Technology Journal*, vol. 38, 2020.

[60] W. S. Cardozo and H. I. Weber, "A compact formulation for constant velocity joint kinematics," *Mechanism and Machine Theory*, vol. 121, pp. 1–14, 2018, doi: 10.1016/j.mechmachtheory.2017.10.009.

[61] S. Sakurai and S. Katsura, "Singularity-free 3-leg 6-dof spatial parallel robot with actuation redundancy," *IEEJ Journal of Industry Applications*, vol. 13, 2024, doi: 10.1541/ieejjia.23003740.

[62] Y. Liu *et al*., "Singularity Analysis and Solutions for the Origami Transmission Mechanism of Fast-Moving Untethered Insect-Scale Robot," in *IEEE Transactions on Robotics*, vol. 40, pp. 777-796, 2024, doi: 10.1109/TRO.2023.3338949.

[63] Y. Li and L. Wang, "Comprehensive research and analysis on obstacle–singularity–joint limit avoidance of redundant robot," *International Journal of Advanced Robotic Systems*, vol. 21, 2024, doi: 10.1177/17298806241233910.

[64] Y. Wang, Y. Liu, M. Leibold, M. Buss and J. Lee, "Hierarchical Incremental MPC for Redundant Robots: A Robust and Singularity-Free Approach," in *IEEE Transactions on Robotics*, vol. 40, pp. 2128-2148, 2024, doi: 10.1109/TRO.2024.3370049.

[65] D. Guo, J. Liu, S. Zheng, J. -P. Cai and P. Jiang, "Singularity-Free Fixed-Time Neuro-Adaptive Control for Robot Manipulators in the Presence of Input Saturation and External Disturbances," in *IEEE Access*, vol. 12, pp. 1794-1804, 2024, doi: 10.1109/ACCESS.2023.3347807.

[66] J. Xu, M. Gao, X. Feng, Z. Tu, S. Zhang, J. Tan, L. Tu, and R. Yao, "Dexterity distribution design for attitude adjustment of multi-joint robotics based on singularity-free workspace decomposition," *Mechanics Based Design of Structures and Machines*, vol. 52, no. 3, 2024, doi: 10.1080/15397734.2022.2162541.

[67] A. Yigit, D. Breton, and C. Gosselin, "Exploiting the kinematic redundancy of a (6 + 3)-degree-of-freedom parallel manipulator to produce unlimited rotation of the platform," *Journal of Mechanisms and Robotics*, vol. 16, no. 7, 2024, 10.1115/1.4063407.

[68] F. Dyba and A. Mazur, "Comparison of curvilinear parametrization methods and avoidance of orthogonal singularities in the path following task," *Journal of Automation, Mobile Robotics and Intelligent Systems*, vol. 17, no. 3, pp. 46–64, 2024, doi: 10.14313/JAMRIS/3-2023/22.

[69] J. Erskine, S. Briot, I. Fantoni and A. Chriette, "Singularity Analysis of Rigid Directed Bearing Graphs for Quadrotor Formations," in *IEEE Transactions on Robotics*, vol. 40, pp. 139-157, 2024, doi: 10.1109/TRO.2023.3324198.

[70] Y. Fan, H. Zhan, Y. Li and C. Yang, "A Predefined Time Constrained Adaptive Fuzzy Control Method With Singularity-Free Switching for Uncertain Robots," in *IEEE Transactions on Fuzzy Systems*, vol. 32, no. 5, pp. 2650-2662, 2024, doi: 10.1109/TFUZZ.2024.3357124.

[71] O. A. Somefun, K. Akingbade, and F. Dahunsi, "The dilemma of pid tuning," *Annual Reviews in Control*, vol. 52, pp. 65–74, 2021, doi: 10.1016/j.arcontrol.2021.05.002.

[72] I. Cervantes and J. Alvarez-Ramirez, "On the pid tracking control of robot manipulators," *Systems and Control Letters*, vol. 42, pp. 37–46, 2001, doi: 10.1016/S0167-6911(00)00077-3.

[73] J. d. J. Rubio, P. Cruz, L. A. Paramo, J. A. Meda, D. Mujica and R. S. Ortigoza, "PID Anti-Vibration Control of a Robotic Arm," in *IEEE Latin America Transactions*, vol. 14, no. 7, pp. 3144-3150, 2016, doi: 10.1109/TLA.2016.7587614.

[74] R. P. Borase, D. K. Maghade, S. Y. Sondkar, and S. N. Pawar, "A review of pid control, tuning methods and applications," *International Journal of Dynamics and Control*, vol. 9, pp. 818–827, 2021, doi: 10.1007/s40435-020-00665-4.

[75] A. M. El-Dalatony, T. Attia, H. Ragheb, and A. M. Sharaf, "Cascaded pid trajectory tracking control for quadruped robotic leg," *International Journal of Mechanical Engineering and Robotics Research*, vol. 12, no. 1, pp. 40–47, 2023, doi: 10.18178/ijmerr.12.1.40-47.

[76] J. Ohri, D. R. Vyas, and P. N. Topno, "Comparison of robustness of pid control and sliding mode control of robotic manipulator," *International Symposium on Devices MEMS, Intelligent Systems & Communication (ISDMISC)*, pp. 5–10, 2011.

[77] H. R. Nohooji, A. Zaraki, and H. Voos, "Actor–critic learning based pid control for robotic manipulators," *Applied Soft Computing*, vol. 151, 2024, doi: 10.1016/j.asoc.2023.111153.

[78] R. G. David, I, "Pid control dynamics of a robotic arm manipulator with two degrees of freedom," *Control de Processos y Robotica*, 2012.

[79] Y. Pan, X. Li and H. Yu, "Efficient PID Tracking Control of Robotic Manipulators Driven by Compliant Actuators," in *IEEE Transactions on Control Systems Technology*, vol. 27, no. 2, pp. 915-922, 2019, doi: 10.1109/TCST.2017.2783339.

[80] N. T. M. Nguyet and D. X. Ba, "A neural flexible pid controller for task-space control of robotic manipulators," *Frontiers in Robotics and AI*, vol. 9, 2023, doi: 10.3389/frobt.2022.975850.

[81] L. Qiao, M. Zhao, C. Wu, T. Ge, R. Fan, and W. Zhang, "Adaptive pid control of robotic manipulators without equality/inequality constraints on control gains," *International Journal of Robust and Nonlinear Control*, vol. 32, no. 18, pp. 9742–9760, 2022, doi: 10.1002/rnc.5849.

[82] E. Sariyildiz, H. Yu, and K. Ohnishi, "A practical tuning method for the robust pid controller with velocity feed-back," *Machines*, vol. 3, no. 3, pp. 208–222, 2015, doi: 10.3390/machines3030208.

[83] A. J. Muñoz-Vázquez, F. Gaxiola, F. Martínez-Reyes, and A. Manzo-Martínez, "A fuzzy fractional-order control of robotic manipulators with pid error manifolds," *Applied Soft Computing Journal*, vol. 83, 2019, doi: 10.1016/j.asoc.2019.105646.

[84] L. Angel and J. Viola, "Fractional order pid for tracking control of a parallel robotic manipulator type delta," *ISA Transactions*, vol. 79, pp. 172–188, 2018, doi: 10.1016/j.isatra.2018.04.010.

[85] L. Angel and J. Viola, "Control performance assessment of fractional-order pid controllers applied to tracking trajectory control of robotic systems," *WSEAS Transactions on Systems and Control*, vol. 17, pp. 62–73, 2022, doi: 10.37394/23203.2022.17.8.

[86] Z. Dachang, D. Baolin, Z. Puchen, and C. Shouyan, "Constant force pid control for robotic manipulator based on fuzzy neural network algorithm," *Complexity*, vol. 2020, 2020, doi: 10.1155/2020/3491845.

[87] K. Shojaei, "A prescribed performance pid control of robotic cars with only posture measurements considering path curvature," *European Journal of Control*, vol. 65, 2022, doi: 10.1016/j.ejcon.2022.100616.

[88] L. Tian, "Intelligent self-tuning of pid control for the robotic testing system for human musculoskeletal joints test," *Annals of Biomedical Engineering*, vol. 32, pp. 899–909, 2004, doi: 10.1023/B:ABME.0000030759.80354.e8.

[89] P. Chotikunnan, R. Chotikunnan, A. Nirapai, A. Wongkamhang, P. Imura, and M. Sangworasil, "Optimizing membership function tuning for fuzzy control of robotic manipulators using pid-driven data techniques," *Journal of Robotics and Control (JRC)*, vol. 4, no. 2, pp. 128–140, 2023, doi: 10.18196/jrc.v4i2.18108.

[90] M. S. Amiri and R. Ramli, "Intelligent trajectory tracking behavior of a multi-joint robotic arm via genetic–swarm optimization for the inverse kinematic solution," *Sensors*, vol. 21, no. 9, 2021, doi: 10.3390/s21093171.

[91] X. Xiang, C. Yu, L. Lapierre, J. Zhang, and Q. Zhang, "Survey on fuzzy-logic-based guidance and control of marine surface vehicles and underwater vehicles," *International Journal of Fuzzy Systems*, vol. 20, pp. 572–586, 2018, doi: 10.1007/s40815-017-0401-3.